

Article

A Disposable Carbon-Based Electrochemical Cell Modified with Carbon Black and Ag/ δ -FeOOH for Non-Enzymatic H₂O₂ Electrochemical Sensing

Wiviane E. R. de Melo¹, Karoline S. Nantes¹, Ana L. H. K. Ferreira¹, Márcio C. Pereira¹, Luiz H. C. Mattoso², Ronaldo C. Faria³ and André S. Afonso^{1,*}

¹ Institute of Science, Engineering and Technology, Federal University of Jequitinhonha and Mucuri Valleys, Teófilo Otoni 39803-371, MG, Brazil; karoline.nantes@ufvjm.edu.br (K.S.N.); marcio.pereira@ufvjm.edu.br (M.C.P.)

² Nanotechnology National Laboratory for Agriculture (LNNA), Embrapa Instrumentação, São Carlos 13560-970, SP, Brazil; luiz.mattoso@embrapa.br

³ Chemistry Department, Federal University of São Carlos, CP 676, São Carlos 13565-905, SP, Brazil; rcfaria@ufscar.br

* Correspondence: andre.afonso@ufvjm.edu.br

Abstract: Hydrogen peroxide (H₂O₂) is an essential analyte for detecting neurodegenerative diseases and inflammatory processes and plays a crucial role in pharmaceuticals, the food industry, and environmental monitoring. However, conventional H₂O₂ detection methods have drawbacks such as lengthy analysis times, high costs, and bulky equipment. Non-enzymatic sensors have emerged as promising alternatives to overcome these limitations. In this research, we introduce a simple, portable, and cost-effective non-enzymatic sensor that uses carbon black (CB) and silver nanoparticle-modified δ -FeOOH (Ag/ δ -FeOOH) integrated into a disposable electrochemical cell (DCell). Scanning electron microscopy (SEM), energy-dispersive X-ray spectroscopy (EDS), and electrochemical impedance spectroscopy (EIS) confirmed successful CB and Ag/ δ -FeOOH immobilization on the DCell working electrode. Electrochemical investigations revealed that the DCell-CB//Ag/ δ -FeOOH sensor exhibited an approximately twofold higher apparent heterogeneous electron transfer rate constant than the DCell-Ag/ δ -FeOOH sensor, capitalizing on CB's advantages. Moreover, the sensor displayed an excellent electrochemical response for H₂O₂ reduction, boasting a low detection limit of 22 μ M and a high analytical sensitivity of 214 μ A mM⁻¹ cm⁻². Notably, the DCell-CB//Ag/ δ -FeOOH sensor exhibited outstanding selectivity for H₂O₂ detection, even in potential interferents such as dopamine, uric acid, and ascorbic acid. Furthermore, the sensor has the right qualities for monitoring H₂O₂ in complex biological samples, as evidenced by H₂O₂ recoveries ranging from 92% to 103% in 10% fetal bovine serum. These findings underscore the considerable potential of the DCell-CB//Ag/ δ -FeOOH sensor for precise and reliable H₂O₂ monitoring in various biomedical and environmental applications.

Keywords: non-enzymatic sensor; Ag/ δ -FeOOH; carbon black; hydrogen peroxide; electrochemical detection



Citation: Melo, W.E.R.d.; Nantes, K.S.; Ferreira, A.L.H.K.; Pereira, M.C.; Mattoso, L.H.C.; Faria, R.C.; Afonso, A.S. A Disposable Carbon-Based Electrochemical Cell Modified with Carbon Black and Ag/ δ -FeOOH for Non-Enzymatic H₂O₂ Electrochemical Sensing. *Electrochem* **2023**, *4*, 523–536. <https://doi.org/10.3390/electrochem4040033>

Academic Editor: Masato Sone

Received: 1 October 2023

Revised: 24 October 2023

Accepted: 10 November 2023

Published: 14 November 2023



Copyright: © 2023 by the authors. Licensee MDPI, Basel, Switzerland. This article is an open access article distributed under the terms and conditions of the Creative Commons Attribution (CC BY) license (<https://creativecommons.org/licenses/by/4.0/>).

1. Introduction

The medical community is dedicated to early disease detection and prevention using new therapies and technologies, considerably improving quality of life and life expectancy, especially for individuals with early signs of cancer or neurological disorders like Parkinson's or Alzheimer's [1,2]. These conditions share the presence of a common role played by reactive oxygen species (ROS), which are generated through the redox reaction of oxygen-containing molecules such as superoxide (O₂^{•-}), hydroxyl (•OH), peroxy radical (ROO•), and hydrogen peroxide (H₂O₂) [3]. While ROS are naturally produced during

normal cellular processes, their concentration tends to rise in some diseases or with chronic inflammation due to cellular metabolism changes. Hydrogen peroxide, as one of the ROS, has been investigated as a disease indicator, with H_2O_2 levels in human blood ranging from 30 to 50 μM [4]. Additionally, H_2O_2 is a by-product of enzyme-catalyzed reactions, enabling the determination of various biological substances such as cholesterol, glucose, lactate, and urate through H_2O_2 analysis [5].

H_2O_2 is a ROS that forms and degrades quickly in natural waters, with a half-life of a few hours. Solar radiation and chromophoric organic matter are the main factors that generate H_2O_2 through photochemical reactions in water. Moreover, direct human activities, such as adding H_2O_2 to aquaculture, or indirect ones, such as introducing photochemically active organic matter as fluorescent brighteners to rivers, can also increase H_2O_2 levels in natural waters [6]. The concentration of H_2O_2 in rivers can range from 4 to 3200 nM [6,7]. High levels of H_2O_2 can be harmful to aquatic life. To measure H_2O_2 , researchers use the Fenton reaction, with benzene as a chemical probe. This reaction generates hydroxyl radicals from H_2O_2 and Fe^{2+} , which then react with benzene to form phenols. H_2O_2 is determined indirectly by measuring the phenols [6].

Accurate determination of H_2O_2 is vital in medicine, the environment, and the pharmaceutical and food industries. Various techniques, including titration, spectrophotometry, chemiluminescence, fluorescence, and chromatography, have been employed for H_2O_2 determination either directly or indirectly. However, these methodologies often suffer from disadvantages such as high costs, lengthy analysis time, and bulky equipment. In contrast, electrochemical methods offer a more advantageous alternative due to their affordability, portability, miniaturization capability, rapid response, reproducibility, and high sensitivity.

An electrochemical sensor is a type of chemical sensor that is widely used. It uses the catalytic activity of enzymes or nanomaterials on a modified surface to generate a signal. One of the main advantages of the electrochemical sensor is that it can be easily handled. Another advantage is that it uses electrical signals for detection, which are a clean and waste-free analytical method. This makes the electrochemical sensor popular for various applications. The electrochemical sensor can be classified into different types, such as amperometric, potentiometric, impedimetric, photoelectrochemical, and electrogenerated chemiluminescence. Amperometric measurement is a common and accurate method that applies a voltage to the electrode surface to trigger the catalytic redox reaction, producing an electrical current proportional to the amount of the analyte present. A critical feature of the sensor is that it can recognize the specific analyte and avoid interference from other substances. This prevents false-positive results. A sensor can detect H_2O_2 effectively by using electrodes modified with nanostructured materials, improving the sensor's sensitivity, specificity, and reproducibility [4].

In electrochemical H_2O_2 sensors, both enzymatic and non-enzymatic approaches have been developed for applications in biological and environmental settings. Enzymatic sensors, despite their widespread use, face challenges like enzyme denaturation due to pH and temperature variations, high costs, and difficulties in proper enzyme immobilization. Conversely, non-enzymatic sensors offer desirable features such as stability and low costs [8]. Researchers have successfully designed sensors with H_2O_2 sensing capabilities using non-enzymatic metal oxide/hydroxide materials. Recently, an all-plastic disposable carbon electrochemical cell modified with silver nanoparticles and $\delta\text{-FeOOH}$ has been developed, demonstrating an excellent electrocatalytic response for H_2O_2 reduction, with a detection limit of 71 μM [9]. $\delta\text{-FeOOH}$, one of the stable phases of iron oxyhydroxide, holds significant potential for various applications, including water treatment, organic pollutant degradation, solar cells, and photocatalysis [10]. While several researchers have explored non-enzymatic sensors that use different iron oxyhydroxide phases [11–14], the utilization of $\delta\text{-FeOOH}$ in non-enzymatic sensors has been limited.

However, carbon-based nanomaterials have been widely used to improve the electrochemical features of non-enzymatic sensors. These nanomaterials possess intrinsic advantages, including a broad surface area and sp^2 carbon structure, resulting in an in-

creased electroactive area and enhanced electron transfer rate [15]. Carbon black (CB) is particularly advantageous among these nanomaterials due to its affordability, high electrical conductivity, and signal amplification capabilities, similar to other commonly used carbon nanomaterials. Various designs of printed carbon electrodes, incorporating carbon-based nanomaterials alone or in combination with other nanomaterials, have been employed for H_2O_2 analysis [16–20]. However, to our knowledge, non-enzymatic sensors modified with CB and $\delta\text{-FeOOH}$ have not yet been developed.

This study presents a novel non-enzymatic sensor for the accurate electrochemical detection of H_2O_2 . The sensor utilizes a disposable electrochemical cell (DCell) with a modified working electrode consisting of CB and Ag/ $\delta\text{-FeOOH}$, significantly enhancing the electrochemical detection of H_2O_2 . Furthermore, we evaluated the sensor performance in biological samples, demonstrating its suitability for reliable H_2O_2 detection.

2. Materials and Methods

2.1. Reagents and Apparatus

The chemicals used in this paper were of analytical grade and used as supplied. Ammonium iron (II) sulfate hexahydrate ($(\text{NH}_4)_2\text{Fe}(\text{SO}_4)_2 \cdot 6\text{H}_2\text{O}$), sodium hydroxide (NaOH), 30% (*v/v*) hydrogen peroxide (H_2O_2) aqueous solution, silver nitrate (AgNO_3), sodium borohydride (NaBH_4), potassium hexacyanoferrate (III), potassium hexacyanoferrate (II) trihydrate, poly(diallyldimethylammonium chloride) (PDDA) (20 wt.% in H_2O), dopamine hydrochloride, ascorbic acid, uric acid, and disinfected fetal bovine serum (FBS) were purchased from Sigma-Aldrich (St. Louis, MO, USA). Carbon Black powder (Grade N347) was purchased from Omsk Carbon Group (Omsk, Russia). Sodium phosphate monobasic (NaH_2PO_4) and sodium phosphate dibasic (Na_2HPO_4) were obtained from Dinâmica Química (Indaiatuba, SP, Brazil), and potassium chloride (KCl), and 37% (*v/v*) hydrogen chloride (HCl) were supplied by Labsynth (Diadema, SP, Brazil). Ultrapure water from a Millipore Direct Q[®] system (Billerica, MA, USA) was used to prepare the working solutions.

The electrochemical tests were performed using a potentiostat/galvanostat (PalmSes4, model PALM-PS4F210, PalmSens, Houten, Netherlands) connected to a computer running PSTRace 5.9 software. The electrochemical transducer was a custom-made disposable plastic electrochemical cell (Dcell) comprising three electrodes integrated into a single strip: a carbon working electrode (WE) with an area of 0.07 cm^2 , an Ag|AgCl reference electrode (RE), and a carbon counter electrode (CE). The fabrication of the DCell followed a previously reported method involving a straightforward procedure utilizing a home cutter printer for prototyping and laminating [21]. The morphology of the films was assessed using scanning electron microscopy (SEM) with a DSM960 microscope (Carl Zeiss, Jena, Germany) equipped with an energy-dispersive X-ray spectrometer (EDS). The $\delta\text{-FeOOH}$ and Ag/ $\delta\text{-FeOOH}$ samples were characterized via N_2 adsorption–desorption measurements using an AUTOSORB 1-Quantachrome system. The surface area was determined using the BET model. The pore size distribution was calculated according to the Barrett–Joyner–Halenda theory.

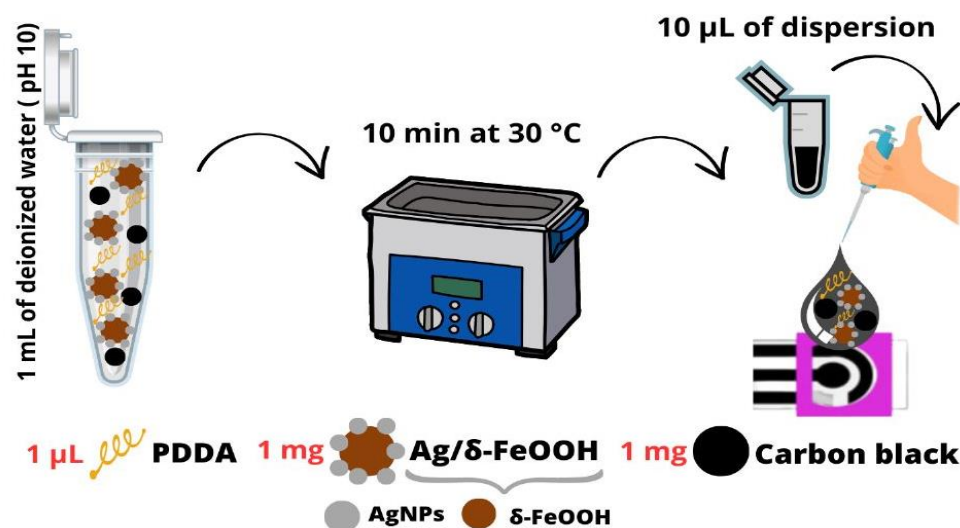
2.2. Synthesis of Ag/ $\delta\text{-FeOOH}$

$\delta\text{-FeOOH}$ was synthesized following a previously reported procedure [9,22]. In brief, 200 mL of 0.71 mM $(\text{NH}_4)_2\text{Fe}(\text{SO}_4)_2 \cdot 6\text{H}_2\text{O}$ solution was mixed with 200 mL of 2 M NaOH solution under mechanical agitation. After forming a green precipitate, 5 mL of 30% H_2O_2 solution was added and stirred for 30 min. The reddish-brown precipitate indicated the production of $\delta\text{-FeOOH}$ particles. The dispersion was thoroughly washed with water to purify the nanoparticles and dried in a vacuum desiccator at room temperature.

Ag/ $\delta\text{-FeOOH}$ was prepared by adding 10 mL of 5% (*m/m*) AgNO_3 solution to a 1.0 g of $\delta\text{-FeOOH}$ dispersion in 25 mL of water. After stirring for 15 min, the mixture was left to stand for 12 h. Subsequently, 30 mg NaBH_4 was added to the solution under stirring for 15 min. The Ag/ $\delta\text{-FeOOH}$ nanocomposite was washed multiple times with water and dried in a vacuum desiccator at room temperature.

2.3. Preparation of the DCell-CB//Ag/ δ -FeOOH Sensor

The working electrode of the DCell was modified by applying a dispersion prepared under optimized conditions. For the preparation, 1 mL of deionized water was utilized, with the pH adjusted to 10 using a NaOH solution. The dispersion consisted of 1 mg of CB, 1 μ L of PDDA, and 1 mg of Ag/ δ -FeOOH. The mixture was ultrasonicated for 10 min at 30 $^{\circ}$ C. Then, 10 μ L of dispersion was drop-cast on the Dcell and air-dried at room temperature (Scheme 1).



Scheme 1. Graphical depiction of the straightforward fabrication process for the DCell-CB//Ag/ δ -FeOOH sensor.

2.4. Electrochemical Characterization

The electrochemical properties of the modified and unmodified DCell were analyzed using cyclic voltammetric (CV) and electrochemical impedance spectroscopy (EIS). The tests were conducted in 1 mM of $K_3Fe(CN)_6$ and 1 mM of $K_4Fe(CN)_6$ in a 0.1 M KCl solution at pH 3.2. For the EIS measurements, an open circuit potential was applied with an amplitude of 5 mV and a frequency range of 100 kHz to 0.01 Hz. To evaluate the electrochemical sensing capabilities of the modified Dcell, CV and amperometry techniques were employed in an N_2 -saturated 0.2 M PBS solution at pH 7.2, with or without H_2O_2 .

3. Results and Discussion

3.1. The Morphological and Electrochemical Characterization of the DCell-CB//Ag/ δ -FeOOH Sensor

Figure 1A presents the SEM image of the DCell-CB//Ag/ δ -FeOOH sensor. The image reveals a well-coated mixture of CB and Ag/ δ -FeOOH on the working electrode, displaying a heterogeneous surface with porous topography. Notably, the modified electrode exhibits increased surface irregularities compared to the unmodified DCell previously reported [21], which can enhance conductivity and its analytical response. The EDS analysis in Figure 1B shows C, Ag, and Fe, validating the successful modification of the DCell's working electrode.

The specific surface areas of pure δ -FeOOH and Ag/ δ -FeOOH were determined from N_2 adsorption–desorption isotherms (Figure 2A). Both samples exhibited a type IV isotherm, characteristic of nanomaterials with interparticle mesoporosity, and an H3 hysteresis loop due to nitrogen capillary condensation within the mesopores. The specific surface area of δ -FeOOH ($94 \text{ m}^2 \text{ g}^{-1}$) is greater than that of Ag/ δ -FeOOH ($63 \text{ m}^2 \text{ g}^{-1}$), suggesting that Ag nanoparticles occupy a portion of the δ -FeOOH pores. The pore-size distribution (Figure 2B) revealed a wide range, from 2 to 60 nm, confirming the mesoporosity of these samples. The pore size distribution profiles of the two samples were similar, except in the 2–4 nm range, where a lower quantity of pores was observed

in the Ag/ δ -FeOOH sample than in δ -FeOOH, confirming the insertion of metallic Ag nanoparticles into the δ -FeOOH pores.

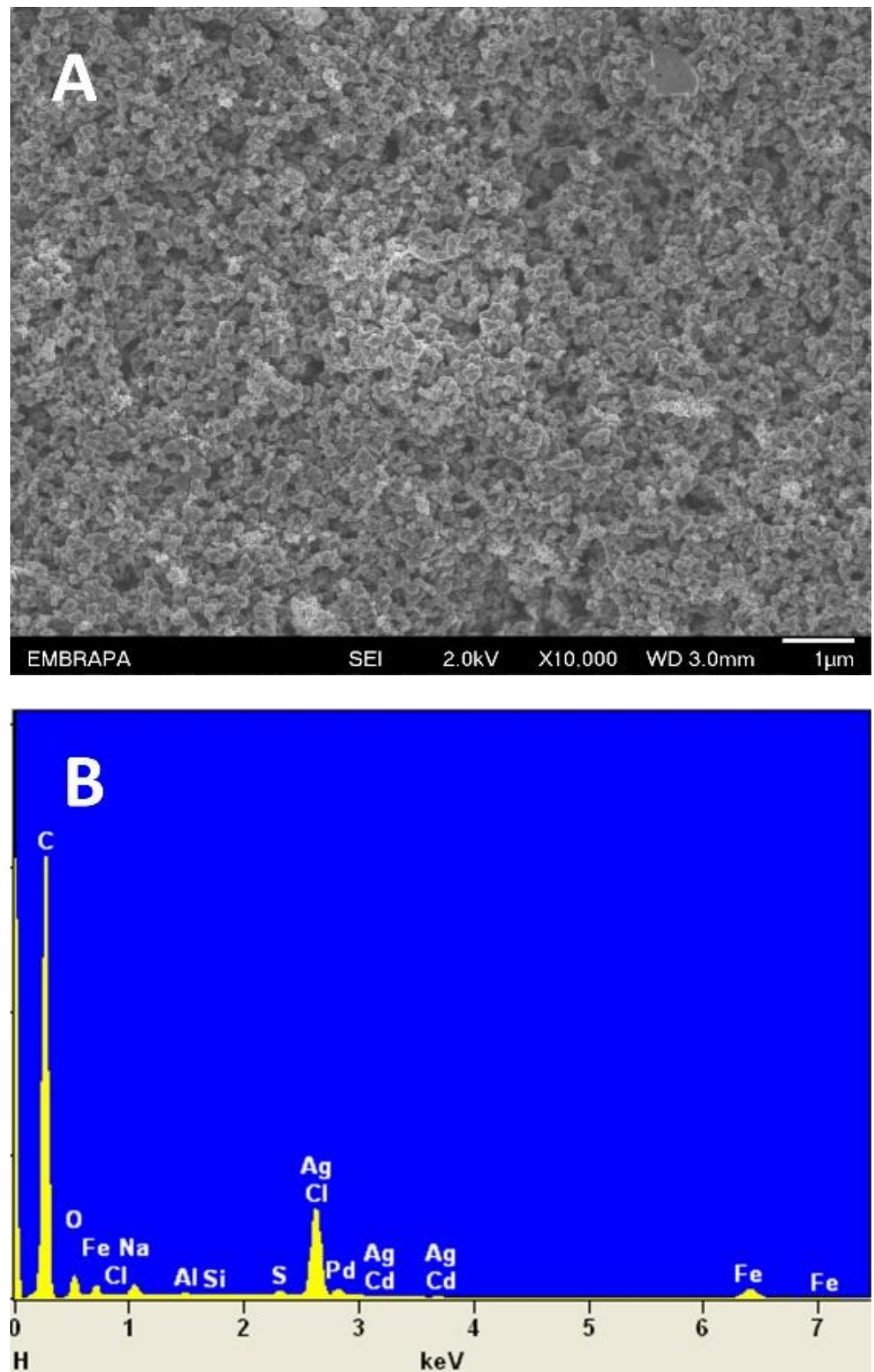


Figure 1. (A) SEM image and (B) EDS spectrum of DCell modified with CB//Ag/ δ -FeOOH.

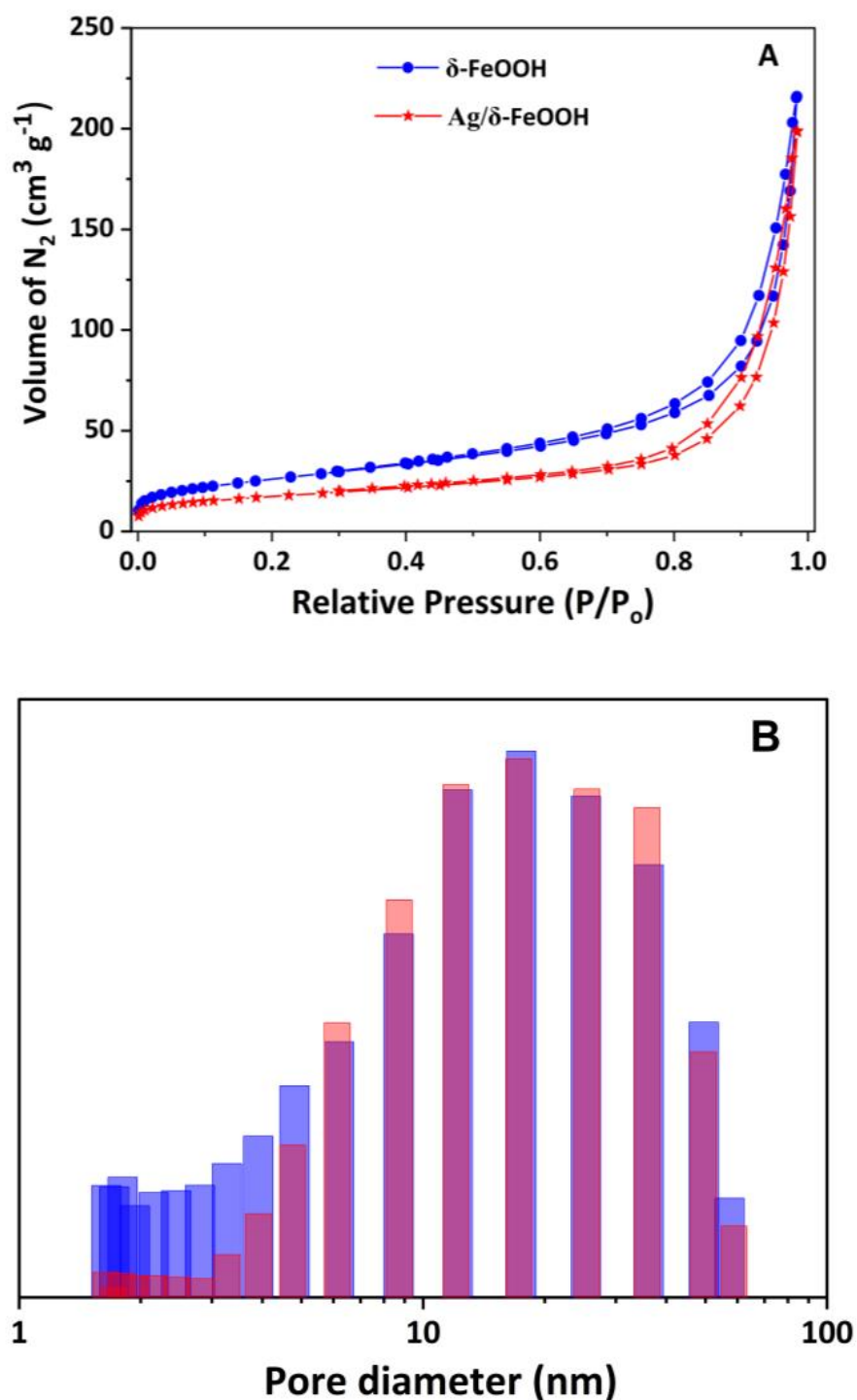


Figure 2. (A) Nitrogen adsorption–desorption isotherms and (B) pore size distribution curves for the δ -FeOOH and Ag/ δ -FeOOH samples. Blue and red bars represent δ -FeOOH and Ag/ δ -FeOOH, respectively.

EIS and CV were used to assess the electrochemical characteristics of the modified and unmodified DCells in a ferri-ferro cyanide solution. Figure 3A shows the EIS spectra for the DCell (a), the DCell modified with Ag/ δ -FeOOH (b), and the DCell modified with CB//Ag/ δ -FeOOH (c). The bare DCell exhibited an Rct of $1.4 \times 10^4 \Omega$, which significantly decreased after modification with Ag/ δ -FeOOH (389 Ω) and CB//Ag/ δ -FeOOH (130 Ω). These findings indicate that Ag/ δ -FeOOH and CB//Ag/ δ -FeOOH play a crucial role as promoters of electron transfer in the ferri/ferro-cyanide redox system at the working

electrode surface. The CV results in Figure 3B align well with the EIS findings. The DCell-CB//Ag/ δ -FeOOH sensor demonstrated a better current response ($I_{\text{oxi}} = 38.10 \mu\text{A}$ and $I_{\text{red}} = -36.31 \mu\text{A}$, $\Delta E_p = 110 \text{ mV}$) compared to the DCell-Ag/ δ -FeOOH ($I_{\text{oxi}} = 18.83 \mu\text{A}$ and $I_{\text{red}} = -23.22 \mu\text{A}$, $\Delta E_p = 110 \text{ mV}$) and the bare DCell sensors ($I_{\text{oxi}} = 7.01 \mu\text{A}$ and $I_{\text{red}} = -7.01 \mu\text{A}$, $\Delta E_p = 270 \text{ mV}$). The ΔE_p value of more than 58 mV (the expected value for a one-electron Nernstian process) suggests a quasi-reversible electrochemical response. The remarkable improvement observed is linked to the particular properties of CB, such as its broad surface area and excellent conductivity [15]. Previous studies have reported that screen-printed electrodes modified with CB via drop-casting exhibit lower peak-to-peak separation and a higher intensity peak current in a ferri-ferro cyanide solution, aligning with our findings [15,23].

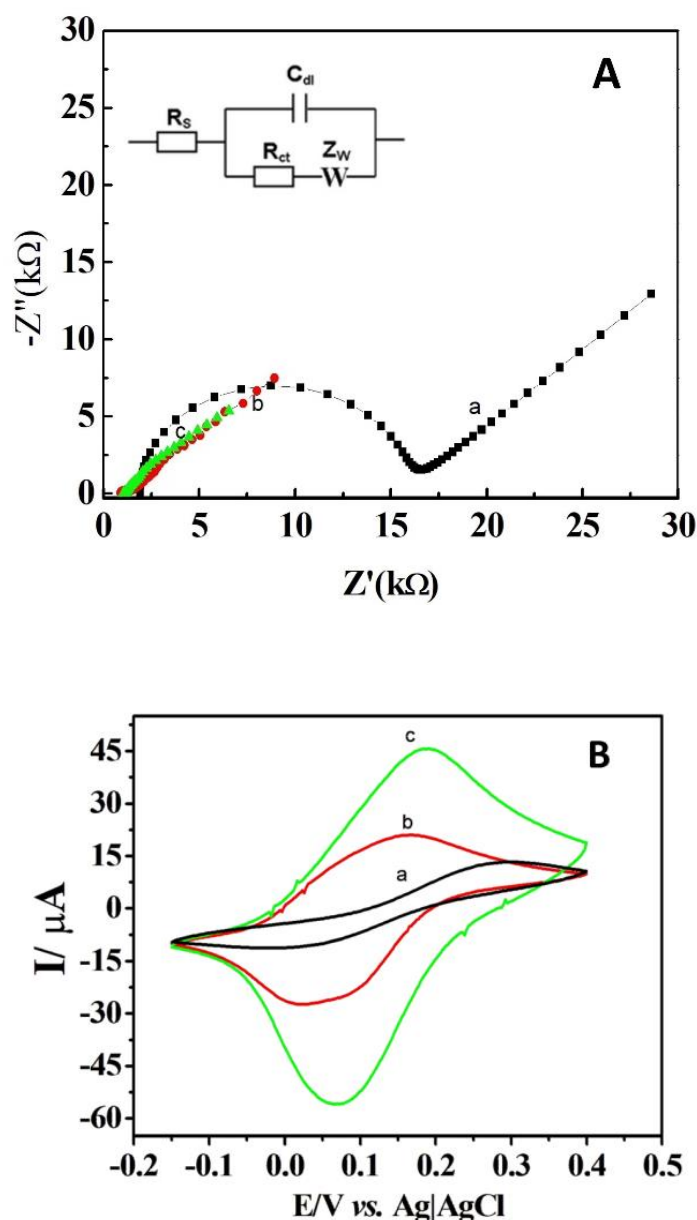


Figure 3. (A) Impedance plots at open-circuit potential and (B) cyclic voltammograms at 100 mV s^{-1} using $1 \text{ mM K}_3\text{Fe(CN)}_6$ and $1 \text{ mM K}_4\text{Fe(CN)}_6$ in $0.1 \text{ M KCl pH } 3.2$ for (a) Dcell, (b) DCell modified with Ag/ δ -FeOOH, and (c) DCell modified with CB//Ag/ δ -FeOOH.

Furthermore, the magnitudes of the voltammetric peak currents plotted against the square root of the applied scan rate ($v^{1/2}$), ranging from $10\text{--}200 \text{ mV s}^{-1}$, exhibited a linear

relationship for the bare DCell, DCell-Ag/ δ -FeOOH, and DCell-CB//Ag/ δ -FeOOH sensors, indicating a diffusion-controlled process at the electrode surface (Figure S1). The apparent heterogeneous electron-transfer rate constant, K_{app}^0 , for the quasi-reversible system, was determined using the Nicholson method [24–26]. The rate constants calculated in the ferri-ferro cyanide solution were $3.21 \times 10^{-4} \pm 9.36 \times 10^{-6} \text{ cm s}^{-1}$, $1.66 \times 10^{-3} \pm 6.10 \times 10^{-5} \text{ cm s}^{-1}$, and $3.06 \times 10^{-3} \pm 1.10 \times 10^{-4} \text{ cm s}^{-1}$, for the bare Dcell, DCell-Ag/ δ -FeOOH, and DCell-CB//Ag/ δ -FeOOH sensors, respectively. These results demonstrate that the DCell-CB//Ag/ δ -FeOOH sensor exhibits a superior performance, with a rate constant approximately twice that of DCell-Ag/ δ -FeOOH. The slower electron transfer rate observed for the bare DCell in the ferri-ferro cyanide solution is consistent with the higher Rct value obtained from the EIS data. Our experimental findings indicate significant improvements in the electrochemical performance of the DCell-CB//Ag/ δ -FeOOH sensor using CB, highlighting the advantages of incorporating CB to enhance the magnitude of K_{app}^0 [15].

Additionally, the working electrode areas for the bare DCell, DCell-Ag/ δ -FeOOH, and DCell-CB//Ag/ δ -FeOOH sensors were determined experimentally using the Randles–Sevcik equation [21,27]. The electroactive areas, evaluated using the ferri-ferro cyanide solution, were found to be $0.021 \pm 0.002 \text{ cm}^2$, $0.190 \pm 0.010 \text{ cm}^2$, and $0.239 \pm 0.009 \text{ cm}^2$, respectively. The DCell modified with CB and Ag/ δ -FeOOH exhibited a larger electroactive area, providing more sites for electrochemical reactions, consistent with the superior electrochemical behavior observed for the DCell-CB//Ag/ δ -FeOOH sensor.

3.2. The Electrochemical Behavior of H_2O_2 in the DCell-CB//Ag/ δ -FeOOH Sensor

Cyclic voltammetry (CV) was employed to investigate the electrochemical attributes of the DCell-CB//Ag/ δ -FeOOH sensor for H_2O_2 reduction. The voltammograms of the DCell (a), DCell-CB (b), DCell-CB// δ -FeOOH (c), and DCell-CB//Ag/ δ -FeOOH sensors (d) in N_2 -saturated 0.2 M PBS at pH 7.2 with 500 μM of H_2O_2 , recorded at a scan rate of 100 mV s^{-1} , are presented in Figure 4A. Curves a and b demonstrate no significant change to H_2O_2 in the -1.0 to 1.0 V range for the DCell and DCell-CB sensors, respectively. Curve c, corresponding to the DCell-CB// δ -FeOOH sensor, shows an anodic current of $16 \mu\text{A}$ and a cathodic current of $19 \mu\text{A}$ at -0.15 V and -0.75 V , respectively, with H_2O_2 added, indicating the redox process of H_2O_2 on δ -FeOOH [9]. Curve d, representing the electrochemical profile of the DCell-CB//Ag/ δ -FeOOH sensor in H_2O_2 solution, displays an anodic current of $134.0 \mu\text{A}$ and $39.4 \mu\text{A}$ at 0.08 V and -0.15 V , respectively, as well as a cathodic current of $100.0 \mu\text{A}$ and $57.0 \mu\text{A}$ at -0.3 V and -0.75 V , respectively.

The sharp oxidation peak at 0.08 V might be related to the oxidation of silver nanoparticles' coverage on δ -FeOOH, and the reduction peak at -0.3 V may arise from the reduction of silver halides or silver oxide formed during the forward scan on δ -FeOOH. Similar observations were reported by Plowman et al. for gold–silver alloy nanoparticles in KCl solution, where an oxidation peak of silver nanoparticles at 0.14 V and a reduction peak at 0.01 V in the reverse scan were associated with the reduction of silver chloride produced in the forward scan [28]. The peak currents at -0.15 V and -0.75 V can be attributed to the redox process of H_2O_2 on the CB//Ag/ δ -FeOOH.

Figure 4B illustrates the voltammograms of the DCell-Ag/ δ -FeOOH (a), DCell-CB//Ag/ δ -FeOOH (b), and DCell-CB sensors (c), along with their respective background voltammograms in N_2 -saturated 0.2 M PBS at pH 7.2, with and without 500 μM H_2O_2 , recorded at a scan rate of 100 mV s^{-1} . Notably, the CB on the working electrode catalyzes the redox process of silver on δ -FeOOH in PBS, leading to anodic and cathodic peaks at 0.08 V and -0.3 V , respectively, which are absent in the voltammograms of the DCell-Ag/ δ -FeOOH and DCell-CB. Furthermore, a 33% increase in the cathodic peak current at -0.75 V in 500 μM H_2O_2 /PBS solution is observed for the DCell-CB//Ag/ δ -FeOOH sensor compared to the DCell-Ag/ δ -FeOOH sensor. These results might be ascribed to the superior electrochemical behavior and higher electroactive area of the working electrode in the DCell-CB//Ag/ δ -FeOOH sensor. The enhancement of the electroanalytical performance for H_2O_2 observed in working electrodes modified with CB has been reported in previous

studies, which indicated an improved electrochemical activity due to the high conductivity and high surface-to-volume ratio provided by CB [29,30].

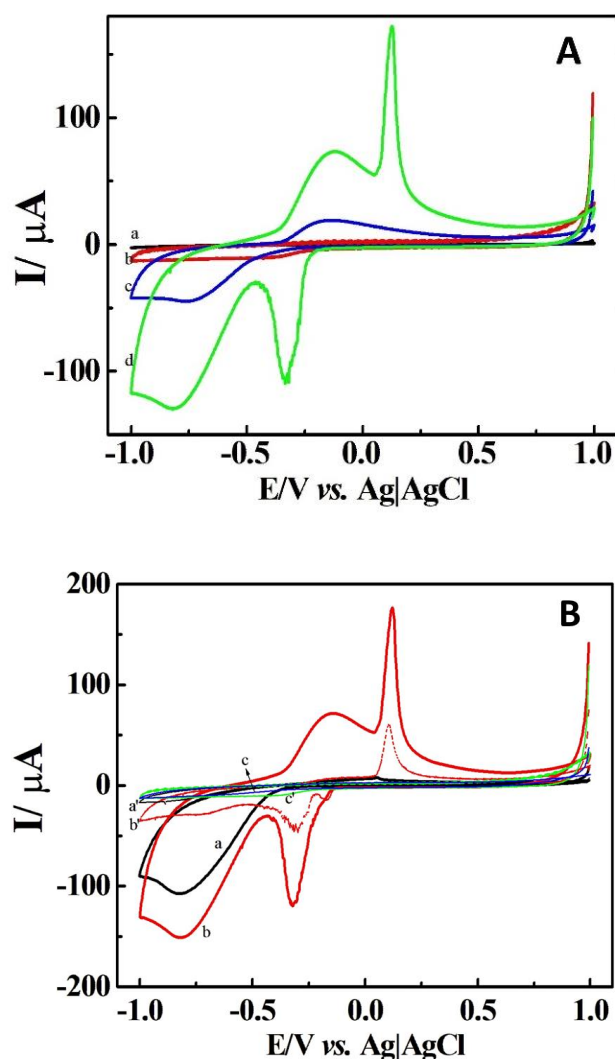


Figure 4. (A) Cyclic voltammograms of DCell (a), DCell-CB (b), DCell-CB// δ -FeOOH (c), and DCell-CB//Ag/ δ -FeOOH sensors (d) and (B) cyclic voltammograms of DCell-Ag/ δ -FeOOH (a), DCell-CB//Ag/ δ -FeOOH (b), and DCell-CB sensors (c) in N_2 -saturated 0.2 M PBS at pH 7.2 with 500 μM H_2O_2 at a scan rate of 100 mVs^{-1} . a', b', and c' represent the background voltammograms.

After confirming that the DCell-CB//Ag/ δ -FeOOH sensor exhibited the best electrochemical characteristics for H_2O_2 detection, we investigated the peak potential of cyclic voltammetry for detecting H_2O_2 at different concentrations. Amperometry measurements were conducted in N_2 -saturated 0.2 M PBS at pH 7.2, under magnetic agitation, using H_2O_2 concentrations of 100, 500, and 1000 μM . As shown in Figure 5, an increase in current is observed at -0.75 V with the increasing H_2O_2 concentration. However, no significant changes in current were observed at -0.3 V , -0.15 V , and 0.08 V , indicating the absence of an electrochemical process for H_2O_2 at those potentials. Consequently, these potentials were not adequate for electroanalysis. Considering the maximum current achieved at -0.75 V , we selected -0.75 V as the voltage potential for H_2O_2 detection using the DCell-CB//Ag/ δ -FeOOH sensor.

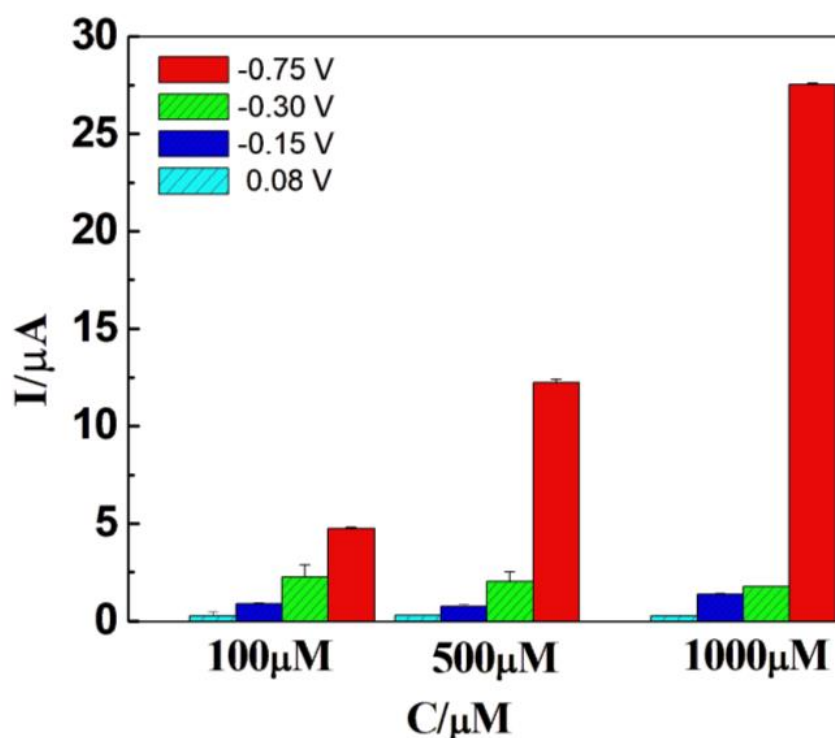
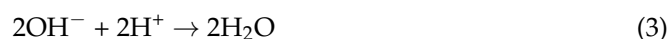


Figure 5. Current responses of Dcell-CB//Ag/δ-FeOOH sensor in N₂-saturated 0.2 M PBS solution (pH 7.2) with 100 μM, 500 μM, or 1000 μM of H₂O₂ at different applied potentials versus Ag|AgCl under magnetic agitation.

Figure 6A depicts the amperometry response of the DCell-CB//Ag/δ-FeOOH sensor at -0.75 V for H₂O₂ detection in N₂-saturated 0.2 M PBS (pH 7.2) under continuous stirring. The response of the DCell-CB//Ag/δ-FeOOH sensor for H₂O₂ reduction is rapid, reaching a steady-state signal quickly upon the addition of H₂O₂. As shown in Figure 6B, the current changes linearly with an increasing H₂O₂ concentration from 70 μM to 6000 μM. Typically, the concentration of H₂O₂ in a human cell is less than 10 nM, and in human plasma, it ranges from 1 to 5 μM. However, during inflammation, the H₂O₂ concentration in plasma can exceed 50 μM [31,32]. In our experiments, the regression equation was $(I/\mu\text{A}) = 0.015 \times [\text{H}_2\text{O}_2] \mu\text{M} - 10$ ($R^2 = 0.997$). The limit of detection (LOD) was calculated to be 22 μM ($S/N = 3$), and the limit of quantification was 70 μM, which reliably covers the concentration range in plasma during inflammation. The sensitivity of the method was $214 \pm 2 \mu\text{A mM}^{-1} \text{cm}^{-2}$. Our results demonstrate that the proposed electroanalytical method exhibits comparable features to those previously reported (see Table S1 [9,33–36]).

A possible explanation of the mechanisms of the electrochemical reduction of H₂O₂ on the surface the DCell-CB//Ag/δ-FeOOH sensor are given in Equations (1)–(3) below. The first step: H₂O₂ receives one electron to form OH[−] and adsorbed OH (OH_{ads}). The second step: OH_(ads) receives one electron to form OH[−]. The third step: the neutralization reaction. The high surface-to-ratio volume provided by CB probably facilitates OH adsorption on the sensor's surface.



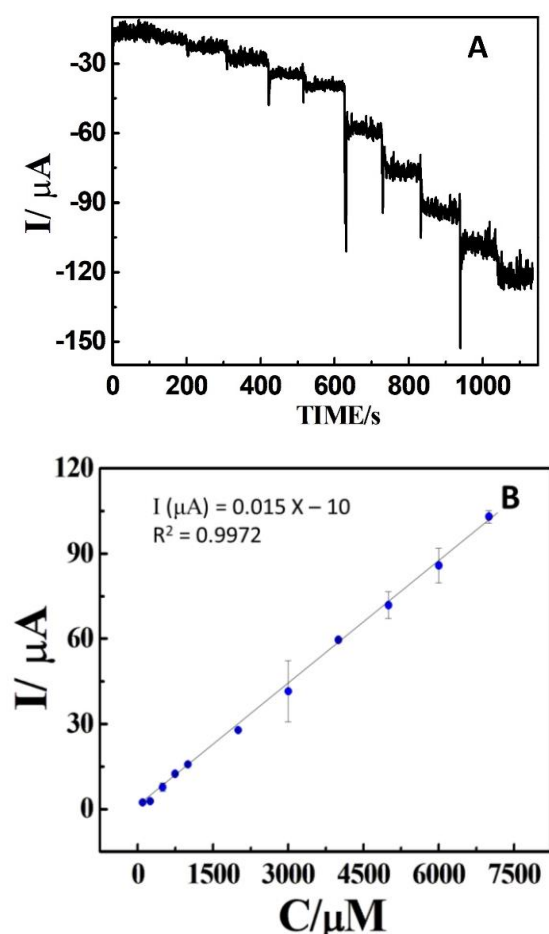


Figure 6. (A) Amperometric results of DCell-CB//Ag/δ-FeOOH sensor to sequential additions of H_2O_2 in N_2 -saturated 0.2 M PBS solution at pH 7.2, recorded at an applied potential of -0.75 V versus Ag|AgCl under magnetic agitation. (B) Corresponding calibration curve. The error bars show the standard deviation for $n = 3$.

3.3. Repeatability, Interference Studies, Storage Stability, and Biological Sample Analysis

We assessed the effectiveness of the DCell-CB//Ag/δ-FeOOH sensor in generating consistent electrochemical results in PBS containing H_2O_2 . For five different DCell-CB//Ag/δ-FeOOH sensor measurements with a peak current average of $53.6 \mu\text{A}$, the relative standard deviation (RSD) was calculated to be about 4.78%, demonstrating the reliability of the fabrication process. Furthermore, we evaluated the interference effects of common biomolecules in physiologic samples, such as ascorbic acid, uric acid, and dopamine [37,38], on the DCell-CB//Ag/δ-FeOOH sensor. Electrochemical measurements (Figure 7) were achieved in N_2 -saturated 0.2 M PBS (pH 7.2) at -0.75 V under continuous stirring. In $100 \mu\text{M}$ of dopamine, uric acid, and ascorbic acid, the DCell-CB//Ag/δ-FeOOH sensor showed no current signal. However, significant amperometric responses were observed upon adding $100 \mu\text{M}$ of H_2O_2 in the initial and final steps. Notably, there was no change in the current signal of H_2O_2 after introducing interfering agents, indicating the excellent selectivity of the proposed sensor. Moreover, the storage stability of the sensor was tested by wrapping it and keeping it at 25°C in a room. The current response of the sensor still maintained 65% of the initial response after seven days. These characteristics, coupled with the reliable response of the DCell-CB//Ag/δ-FeOOH sensor, make it suitable for detecting H_2O_2 levels in biological samples.

Fetal bovine serum (FBS) is commonly added as a supplement to the basal medium in cell culture. Cells can release H_2O_2 when stimulated in a cell culture medium containing 10% fetal bovine serum [39,40]. Therefore, sensing performance for application in biological

samples can be assessed in a solution containing FBS. To this end, we applied the DCell-CB//Ag/ δ -FeOOH sensor to determine the H_2O_2 levels in a 10% fetal bovine serum disinfected solution diluted in 0.2 M PBS (pH 7.2). The samples were spiked with different concentrations of H_2O_2 standard solution (Table 1). The calculated H_2O_2 recoveries fell within the range of 92 to 103%. These results highlight the potential of the DCell-CB//Ag/ δ -FeOOH sensor for monitoring H_2O_2 in biological samples.

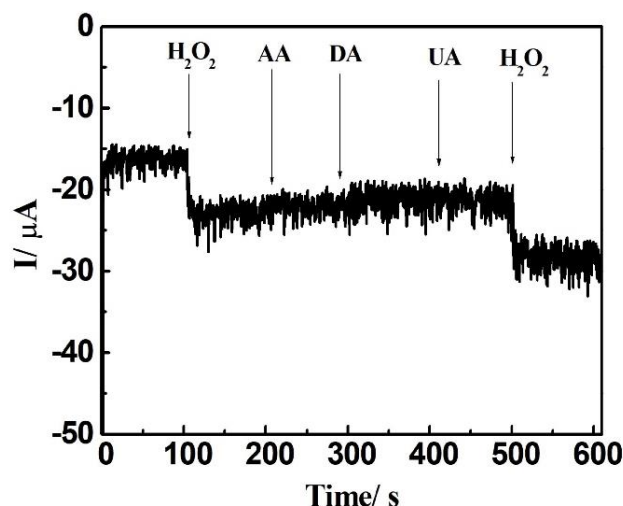


Figure 7. Amperometric results of Dcell-CB//Ag/ δ -FeOOH sensor using 100 μM H_2O_2 (initial and final additions) and 100 μM of ascorbic acid (AA), dopamine (DA), uric acid (UA) in N_2 -saturated 0.2 PBS at pH 7.2, recorded at -0.75 V versus Ag|AgCl under continuous stirring.

Table 1. Spiking and recovery of H_2O_2 in 10% of fetal bovine serum diluted in PBS.

Sample	Added (μM)	Found (μM)	Recovery (μM)
1	500	515.6	103%
2	2000	1834.5	92%

4. Conclusions

We developed a non-enzymatic sensor using a carbon black (CB) and Ag/ δ -FeOOH composite for H_2O_2 detection. The effective immobilization of the CB and Ag/ δ -FeOOH composite onto the DCell working electrode was confirmed through SEM, EDS, and EIS analyses. BET analysis confirmed the insertion of metallic Ag nanoparticles into the δ -FeOOH pores. Thus, the incorporation of CB into the DCell-CB//Ag/ δ -FeOOH sensor resulted in a significant improvement in its electrochemical performance, leveraging the unique properties of CB. Specifically, the apparent rate constant of heterogeneous electron transfer in the DCell-CB//Ag/ δ -FeOOH sensor was nearly doubled compared to that of the DCell-Ag/ δ -FeOOH sensor. Our sensor demonstrated exceptional sensitivity, reproducibility, and selectivity for electrochemical H_2O_2 detection. Furthermore, the successful application of the sensor in the electroanalytical assay of 10% fetal bovine serum highlighted its potential for precise H_2O_2 detection in complex biological samples. These findings emphasize the promising potential of the DCell-CB//Ag/ δ -FeOOH sensor in advancing electrochemical sensing technologies for diverse biomedical and environmental purposes.

Supplementary Materials: The following supporting information can be downloaded at <https://www.mdpi.com/article/10.3390/electrochem4040033/s1>. Figure S1: Cyclic voltammograms resulting from increasing scan rate (10–200 mV s^{-1}) and plot peak current versus square root of the scan rate at DCell (A and B) and DCell modified with Ag/ δ -FeOOH (C and D) and DCell modified with CB//Ag/ δ -FeOOH (E and F) in 1 mM of $\text{K}_3\text{Fe}(\text{CN})_6$ and 1 mM of $\text{K}_4\text{Fe}(\text{CN})_6$ in 0.1 M KCl pH 3.2. Table S1. LOD values for other modified electrodes for H_2O_2 detection.

Author Contributions: W.E.R.d.M.: conceptualization, methodology, experimental work, data analysis, and writing—original draft; K.S.N. and A.L.H.K.F.: methodology and experimental work; M.C.P.: resource and writing—review and editing; L.H.C.M. and R.C.F.: methodology, experimental work, and resources; A.S.A.: conceptualization, supervision, methodology, data analysis, resources, and writing—review and editing. All authors have read and agreed to the published version of the manuscript.

Funding: This research was funded by FAPEMIG (APQ-00607-22).

Institutional Review Board Statement: Not applicable.

Informed Consent Statement: Not applicable.

Data Availability Statement: The data presented in this study are available on request from the corresponding author.

Acknowledgments: We thank FAPEMIG, CNPq, and FINEP/MCTI for their support. We also acknowledge the Institute of Science, Engineering, and Technology of the Federal University of Jequitinhonha and Mucuri Valleys for supporting this work.

Conflicts of Interest: The authors declare no conflict of interest.

References

1. Berg, D. Biomarkers for the early detection of Parkinson's and Alzheimer's disease. *Neurodegener. Dis.* **2008**, *5*, 133–136. [[CrossRef](#)] [[PubMed](#)]
2. Pepe, M.S.; Etzioni, R.; Feng, Z.D.; Potter, J.D.; Thompson, M.L.; Thornquist, M.; Winget, M.; Yasui, Y. Phases of biomarker development for early detection of cancer. *J. Natl. Cancer Inst.* **2001**, *93*, 1054–1061. [[CrossRef](#)] [[PubMed](#)]
3. Deshpande, A.S.; Muraoka, W.; Andreescu, S. Electrochemical sensors for oxidative stress monitoring. *Curr. Opin. Electrochem.* **2021**, *29*, 10. [[CrossRef](#)]
4. Geraskevich, A.V.; Solomonenko, A.N.; Dorozhko, E.V.; Korotkova, E.I.; Berek, J. Electrochemical Sensors for the Detection of Reactive Oxygen Species in Biological Systems: A Critical Review. *Crit. Rev. Anal. Chem.* **2022**. [[CrossRef](#)] [[PubMed](#)]
5. Chen, X.M.; Wu, G.H.; Cai, Z.X.; Oyama, M.; Chen, X. Advances in enzyme-free electrochemical sensors for hydrogen peroxide, glucose, and uric acid. *Microchim. Acta* **2014**, *181*, 689–705. [[CrossRef](#)]
6. Sunday, M.O.; Jadoon, W.A.; Ayeni, T.T.; Iwamoto, Y.; Takeda, K.; Imaizumi, Y.; Arakaki, T.; Sakugawa, H. Heterogeneity and potential aquatic toxicity of hydrogen peroxide concentrations in selected rivers across Japan. *Sci. Total Environ.* **2020**, *733*, 9. [[CrossRef](#)]
7. Giaretta, J.E.; Duan, H.W.; Oveissi, F.; Farajikhah, S.; Dehghani, F.; Naficy, S. Flexible Sensors for Hydrogen Peroxide Detection: A Critical Review. *ACS Appl. Mater. Interfaces* **2022**, *14*, 20491–20505. [[CrossRef](#)]
8. Thatikayala, D.; Ponnamma, D.; Sadasivuni, K.K.; Cabibihan, J.J.; Al-Ali, A.K.; Malik, R.A.; Min, B. Progress of Advanced Nanomaterials in the Non-Enzymatic Electrochemical Sensing of Glucose and H₂O₂. *Biosensors* **2020**, *10*, 151. [[CrossRef](#)]
9. de Meira, F.H.A.; Resende, S.F.; Monteiro, D.S.; Pereira, M.C.; Mattoso, L.H.C.; Faria, R.C.; Afonso, A.S. A Non-enzymatic Ag/delta-FeOOH Sensor for Hydrogen Peroxide Determination using Disposable Carbon-based Electrochemical Cells. *Electroanalysis* **2020**, *32*, 2231–2236. [[CrossRef](#)]
10. Huang, Z.X.; Han, F.S.; Li, M.T.; Zhou, Z.H.; Guan, X.J.; Guo, L.J. Which phase of iron oxyhydroxides (FeOOH) is more competent in overall water splitting as a photocatalyst, goethite, akaganeite or lepidocrocite? A DFT-based investigation. *Comput. Mater. Sci.* **2019**, *169*, 8. [[CrossRef](#)]
11. Zhang, N.; Sheng, Q.L.; Zhou, Y.Z.; Dong, S.Y.; Zheng, J.B. Synthesis of FeOOH@PDA-Ag nanocomposites and their application for electrochemical sensing of hydrogen peroxide. *J. Electroanal. Chem.* **2016**, *781*, 315–321. [[CrossRef](#)]
12. Zhang, J.; Zheng, J.B. An enzyme-free hydrogen peroxide sensor based on Ag/FeOOH nanocomposites. *Anal. Methods* **2015**, *7*, 1788–1793. [[CrossRef](#)]
13. Zhao, C.L.; Zhang, H.F.; Zheng, J.B. Synthesis of silver decorated sea urchin-like FeOOH nanocomposites and its application for electrochemical detection of hydrogen peroxide. *J. Mater. Sci.-Mater. Electron.* **2017**, *28*, 14369–14376. [[CrossRef](#)]
14. Huang, Y.L.; Liang, G.Z.; Lin, T.R.; Hou, L.; Ye, F.G.; Zhao, S.L. Magnetic Cu/Fe₃O₄@FeOOH with intrinsic HRP-like activity at nearly neutral pH for one-step biosensing. *Anal. Bioanal. Chem.* **2019**, *411*, 3801–3810. [[CrossRef](#)] [[PubMed](#)]
15. Arduini, F.; Cinti, S.; Mazzaracchio, V.; Scognamiglio, V.; Amine, A.; Moscone, D. Carbon black as an outstanding and affordable nanomaterial for electrochemical (bio)sensor design. *Biosens. Bioelectron.* **2020**, *156*, 16. [[CrossRef](#)]
16. Cinti, S.; Arduini, F. Graphene-based screen-printed electrochemical (bio)sensors and their applications: Efforts and criticisms. *Biosens. Bioelectron.* **2017**, *89*, 107–122. [[CrossRef](#)]
17. Ahmad, K.; Kim, H. Fabrication of Nitrogen-Doped Reduced Graphene Oxide Modified Screen Printed Carbon Electrode (N-rGO/SPCE) as Hydrogen Peroxide Sensor. *Nanomaterials* **2022**, *12*, 14. [[CrossRef](#)]

18. He, G.W.; Jiang, J.Q.; Wu, D.; You, Y.L.; Yang, X.; Wu, F.; Hu, Y.J. A Novel Non-enzymatic Hydrogen Peroxide Electrochemical Sensor Based on Facile Synthesis of Copper Oxide Nanoparticles Dopping into Graphene Sheets@Cerium Oxide Nanocomposites Sensitized Screen Printed Electrode. *Int. J. Electrochem. Sci.* **2016**, *11*, 8486–8498. [[CrossRef](#)]
19. Hu, Y.; Hojamberdiev, M.; Geng, D.S. Recent advances in enzyme-free electrochemical hydrogen peroxide sensors based on carbon hybrid nanocomposites. *J. Mater. Chem. C* **2021**, *9*, 6970–6990. [[CrossRef](#)]
20. Yang, X.; Ouyang, Y.J.; Wu, F.; Hu, Y.J.; Zhang, H.F.; Wu, Z.Y. In situ & controlled preparation of platinum nanoparticles dopping into graphene sheets@cerium oxide nanocomposites sensitized screen printed electrode for non-enzymatic electrochemical sensing of hydrogen peroxide. *J. Electroanal. Chem.* **2016**, *777*, 85–91. [[CrossRef](#)]
21. Afonso, A.S.; Uliana, C.V.; Martucci, D.H.; Faria, R.C. Simple and rapid fabrication of disposable carbon-based electrochemical cells using an electronic craft cutter for sensor and biosensor applications. *Talanta* **2016**, *146*, 381–387. [[CrossRef](#)] [[PubMed](#)]
22. Pereira, M.C.; Garcia, E.M.; da Silva, A.C.; Lorencon, E.; Ardisson, J.D.; Murad, E.; Fabris, J.D.; Matencio, T.; Ramalho, T.D.; Rocha, M.V.J. Nanostructured delta-FeOOH: A novel photocatalyst for water splitting. *J. Mater. Chem.* **2011**, *21*, 10280–10282. [[CrossRef](#)]
23. Arduini, F.; Di Nardo, F.; Amine, A.; Micheli, L.; Palleschi, G.; Moscone, D. Carbon Black-Modified Screen-Printed Electrodes as Electroanalytical Tools. *Electroanalysis* **2012**, *24*, 743–751. [[CrossRef](#)]
24. Nicholson, R.S. THEORY AND APPLICATION OF CYCLIC VOLTAMMETRY FOR MEASUREMENT OF ELECTRODE REACTION KINETICS. *Anal. Chem.* **1965**, *37*, 1351–1355. [[CrossRef](#)]
25. Moore, K.E.; Flavel, B.S.; Ellis, A.V.; Shapter, J.G. Comparison of double-walled with single-walled carbon nanotube electrodes by electrochemistry. *Carbon* **2011**, *49*, 2639–2647. [[CrossRef](#)]
26. Muhammad, H.; Tahiri, I.A.; Muhammad, M.; Masood, Z.; Versiani, M.A.; Khaliq, O.; Latif, M.; Hanif, M. A comprehensive heterogeneous electron transfer rate constant evaluation of dissolved oxygen in DMSO at glassy carbon electrode measured by different electrochemical methods. *J. Electroanal. Chem.* **2016**, *775*, 157–162. [[CrossRef](#)]
27. Paixao, T. Measuring Electrochemical Surface Area of Nanomaterials versus the Randles-Sevcik Equation. *Chemelectrochem* **2020**, *7*, 3414–3415. [[CrossRef](#)]
28. Plowman, B.J.; Sidhureddy, B.; Sokolov, S.V.; Young, N.P.; Chen, A.C.; Compton, R.G. Electrochemical Behavior of Gold-Silver Alloy Nanoparticles. *Chemelectrochem* **2016**, *3*, 1039–1043. [[CrossRef](#)]
29. Faisal, M.; Alam, M.M.; Asiri, A.M.; Alsaiani, M.; Alruwais, R.S.; Jalalah, M.; Madkhali, O.; Rahman, M.M.; Harraz, F.A. Detection of hydrogen peroxide with low-dimensional silver nanoparticle-decorated PPy-C/TiO₂ nanocomposites by electrochemical approach. *J. Electroanal. Chem.* **2023**, *928*, 11. [[CrossRef](#)]
30. Liu, Y.Y.; Li, H.M.; Gong, S.P.; Chen, Y.N.; Xie, R.R.; Wu, Q.Q.; Tao, J.; Meng, F.L.; Zhao, P. A novel non-enzymatic electrochemical biosensor based on the nanohybrid of bimetallic PdCu nanoparticles/carbon black for highly sensitive detection of H₂O₂ released from living cells. *Sens. Actuator B-Chem.* **2019**, *290*, 249–257. [[CrossRef](#)]
31. Forman, H.J.; Bernardo, A.; Davies, K.J.A. What is the concentration of hydrogen peroxide in blood and plasma? *Arch. Biochem. Biophys.* **2016**, *603*, 48–53. [[CrossRef](#)] [[PubMed](#)]
32. Wang, Z.; Hong, Y.L.; Li, J.B.; Liu, J.L.; Jiang, H.; Sun, L.N. Upconversion luminescent sensor for endogenous H₂O₂ detection in cells based on the inner filter effect of coated silver layer. *Sens. Actuator B-Chem.* **2023**, *376*, 8. [[CrossRef](#)]
33. Du, S.C.; Ren, Z.Y.; Wu, J.; Xi, W.; Fu, H.G. Vertical alpha-FeOOH nanowires grown on the carbon fiber paper as a free-standing electrode for sensitive H₂O₂ detection. *Nano Res.* **2016**, *9*, 2260–2269. [[CrossRef](#)]
34. Ahmed, J.; Faisal, M.; Jalalah, M.; Alsaiani, M.; Alsareii, S.A.; Harraz, F.A. An efficient amperometric catechol sensor based on novel polypyrrole-carbon black doped alpha-Fe₂O₃ nanocomposite. *Colloid Surf. A-Physicochem. Eng. Asp.* **2021**, *619*, 12. [[CrossRef](#)]
35. Ates, A.; Oskay, K.O. Preparation and characterization of nanosized Fe₃O₄-biochar electrocatalysts with large surface area for H₂O₂ sensing. *Surf. Interfaces* **2022**, *29*, 14. [[CrossRef](#)]
36. Sobahi, N.; Imran, M.; Khan, M.E.; Mohammad, A.; Alam, M.M.; Yoon, T.; Mehedi, I.M.; Hussain, M.A.; Abdulaal, M.J.; Jiman, A.A. Electrochemical Sensing of H₂O₂ by Employing a Flexible Fe₃O₄/Graphene/Carbon Cloth as Working Electrode. *Materials* **2023**, *16*, 2770. [[CrossRef](#)]
37. Chakraborty, P.; Dhar, S.; Debnath, K.; Majumder, T.; Mondal, S.P. Non-enzymatic and non-invasive glucose detection using Au nanoparticle decorated CuO nanorods. *Sens. Actuator B-Chem.* **2019**, *283*, 776–785. [[CrossRef](#)]
38. Waldiya, M.; Bhagat, D.; Narasimman, R.; Singh, S.; Kumar, A.; Ray, A.; Mukhopadhyay, I. Development of highly sensitive H₂O₂ redox sensor from electrodeposited tellurium nanoparticles using ionic liquid. *Biosens. Bioelectron.* **2019**, *132*, 319–325. [[CrossRef](#)]
39. Mao, X.X.; Liu, S.W.; Su, B.Y.; Wang, D.J.; Huang, Z.; Li, J.; Zhang, Y.G. Luminescent europium(III)-organic framework for visual and on-site detection of hydrogen peroxide via a tablet computer. *Microchim. Acta* **2020**, *187*, 11. [[CrossRef](#)]
40. van der Valk, J. Fetal bovine serum—a cell culture dilemma. *Science* **2022**, *375*, 143–144. [[CrossRef](#)]

Disclaimer/Publisher’s Note: The statements, opinions and data contained in all publications are solely those of the individual author(s) and contributor(s) and not of MDPI and/or the editor(s). MDPI and/or the editor(s) disclaim responsibility for any injury to people or property resulting from any ideas, methods, instructions or products referred to in the content.